J Appl Electrochem (2012) 42:341–348
DOI 10.1007/s10800-012-0402-8

ORIGINAL PAPER

Novel bismuth/multi-walled carbon nanotubes-based electrochemical sensor for the determination of neuroprotective drug cilostazol

Rajeev Jain · Ramkishor Sharma

Received: 5 January 2012 / Accepted: 15 March 2012 / Published online: 30 March 2012
© Springer Science+Business Media B.V. 2012

Abstract A very sensitive electrochemical sensor has been developed by modification of glassy carbon electrode (GCE) with nanoparticles of bismuth (III) oxide (Bi_2O_3) and multi-walled carbon nanotubes (MWCNTs). The sensor was applied for the determination of cilostazol, cyclic nucleotide phosphodiesterase inhibitors in pharmaceutical formulation and human plasma. The voltammetric responses were compared with those obtained at bare GCE under optimum conditions. The cyclic and square-wave voltammograms of cilostazol showed 3.3 and 4.9 times enhancement in the oxidation peak current at MWCNTs–Bi_2O_3/GCE as compared to a bare GCE. Bi_2O_3–MWCNTs/GCE showed a linear response for cilostazol in standard solution over the concentration range of 0.8–13 μg mL^{-1} with the detection limit 0.76 μg mL^{-1}, whereas human plasma over the concentration range 0.8–12.5 μg mL^{-1} with the detection limit 0.66 μg mL^{-1}.

Keywords Sensor · Cilostazol · Voltammetry · Pharmaceutical formulation · Human matrix

1 Introduction

In recent years, the fabrication of chemically modified electrode (CME) is widely reported to improve sensitivity and selectivity in the analysis of DNA, amino acid, vitamin, pharmaceuticals, etc. [1–4]. Bismuth oxide is an environmentally friendly element, with very low toxicity and widespread pharmaceutical use [5]. Bismuth oxide is also known to be an important transition metal oxide due to its characteristic parameters such as energy band gap and photoconductivity that are suitable for large range applications [6, 7]. Over the last few years, bismuth has been established as the most promising substitute for mercury in stripping analysis due to high electrical conductivity, chemical stability, and mechanical strength [8–10] and has found a wide range of interesting environmental and clinical applications in trace metal analysis in combination with advanced electrochemical stripping techniques [11–23]. On the other hand, only few reports are available on the use of bismuth film electrodes (BiFEs) for determination of pharmaceuticals [3, 10, 24, 25].

The wide choice of MWCNTs as a nanomaterial in electroanalytical studies of pharmaceutical molecules, ions and toxic compounds gained also interest due to its high electrical conductivity, chemical stability, and mechanical strength [2, 26–30]. These properties indicated that CNT has a fast electron transfer reaction when used as an electrode modifying material [31, 32]. In addition, CNT based-electrodes also showed high sensitivity with good detection limits [33].

Cilostazol, 6-(4-(1-cyclohexyl-1H-tetrazol-5-yl) butoxy)-3,4-dihydro-2(1H)-quinolinone (Scheme 1), is used for the treatment of intermittent claudication and stroke prevention in US, UK, and Japan [34]. Cilostazol is a cyclic nucleotide phosphodiesterase III (PDE III) inhibitor that has antiplatelet, antithrombotic, and vasodilating properties and also exhibits antiproliferative effects on smooth muscle cells [35]. Cilostazol is effective in reducing occurrence of cerebral infarction in diabetic subjects and high-density lipoprotein cholesterol and triglyceride levels [36–40].

The widespread use of this compound and the need for clinical and pharmacological studies required fast and sensitive analytical techniques for the assay of drug in pharmaceutical formulations, biological matrixes, and also for toxicological and pharmacokinetic studies. Several methods

R. Jain (✉) · R. Sharma
School of Studies in Chemistry, Jiwaji University, Gwalior 474011, MP, India
e-mail: rajeevjain54@yahoo.co.in

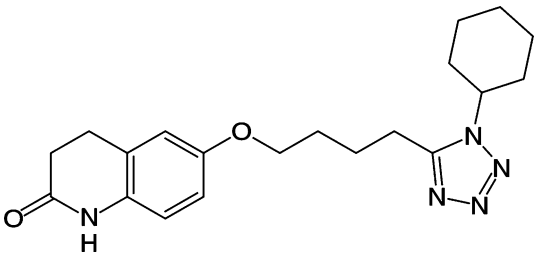

Scheme 1 Chemical structure of cilostazol

have been reported for assay of cilostazol in pharmaceutical formulation and biological fluids including, reverse phase high-performance liquid chromatographic (RP-HPLC) methods [41–43], and liquid chromatography/electrospray tandem mass spectrometry method [40]. These techniques are very time consuming and the demand of expensive, sophisticated instrumentation and highly skilled personnel restrict their use in routine analysis. Since the last decade, electroanalytical techniques have been widely used in the field of pharmaceuticals analysis [44–50], as these techniques are inexpensive, rapid, and do not require time consuming purification steps after extraction, when compared with other analytical techniques [40–43]. However, no electroanalytical methods have yet been reported for the quantification of cilostazol in pharmaceutical formulations and human plasma. The purpose of the present voltammetric studies is to establish the methodology for the detection and quantification of cilostazol using modified electrodes.

However, it is evident that a practical application of bismuth and MWCNTs-modified electrodes in the area of drug analysis is still generally unexplored. In this paper Bi_2O_3, MWCNTs, and mixture of both Bi_2O_3–MWCNTs are used to construct the modified electrodes. The electrochemical characteristics of the modified electrodes were characterized by scanning electron microscopy (SEM). The proposed electrochemical sensor was successfully applied for the detection and quantification of cilostazol in pharmaceutical formulation and human matrix.

2 Experimental section

2.1 Apparatus

All Electrochemical measurements were carried out at μ-Autolab Type III potentiostat–galvanostat (Eco-Chemie B.V., Utrecht, The Netherlands) with 757VA computrace software. The utilized electrodes were GCE, Bi_2O_3/GCE, MWCNTs/GCE, and Bi_2O_3–MWCNTs/GCE as working electrodes, platinum wire as an auxiliary electrode, and Ag/AgCl (3 M KCl) as reference electrode. All pH measurements were performed on a Decibel DB-1011 digital pH meter fitted with a glass electrode as a working electrode and saturated calomel as a reference electrode, which was previously standardized with buffer solutions of known pH.

2.2 Reagents and chemicals

Bi_2O_3 (>99.8 % purity) nanopowder (90–210 nm,) and MWCNTs (>95 % purity) with outer diameter 10–20 nm, internal diameter 5–10 nm, and tube length 0.5–50 μm were procured from Sigma Aldrich. Cilostazol standard (99.23 % purity) was provided by Cadila Pharmaceuticals Ltd., (India). Tablets containing cilostazol (Pletoz® 50 mg/Tab) manufactured by Cipla Ltd., were obtained from commercial source. Ultra-pure water, obtained from Milli-Q purification system (Millipore Corp., Milford, MA, USA). All chemicals used in the study were of analytical reagent grade and employed without further purification.

2.3 Analytical procedure

Standard stock solution of cilostazol (1 mg mL^{-1}) was prepared by dissolving pure compound in acetonitrile and further diluted with same solvents to get final concentration in the working range (0.8–13 μg mL^{-1}). Different human plasma lots were procured from Radha Swami blood bank, Gwalior, India. Plasma was obtained from whole blood anti-coagulated with K_3EDTA. All plasma lots were preserved at −20 °C in freezer and used after gentle thawing at room temperature. Plasma calibrator samples were prepared by 5 % spiking of different concentration of cilostazol (0.8–12.5 μg mL^{-1}) in plasma. Analyte was separated from spiked plasma samples through single step protein precipitation by acetonitrile followed by centrifugation. A series of Britton–Robinson (BR) buffer (2.0–12.0 pH) was prepared in ultra-pure water and used as supporting electrolytes. For electrochemical measurements, a known volume of the analyte samples (standard solution and extracted plasma samples) were pipetted in voltammetric cell and total volume made up to 10 mL with supporting electrolytes; this solution was deoxygenated with pure nitrogen gas for 25 s. The voltammograms were recorded by applying positive potential scan from 0.2–1.6 V (vs. Ag/AgCl), frequency 50 Hz, pulse amplitude 50 mV s^{-1}, and scan increment 10 mV s^{-1}. All measurements were carried out at room temperature.

2.4 Fabrication of Bi_2O_3, MWCNTs, and Bi_2O_3–MWCNTs-modified glassy carbon electrode

To provide a reproducible electrode surface before modification, the bare working electrode (GCE) was cleaned mechanically with alumina powder of different particle sizes (0.05–0.3 μm) suspended in deionised water on a

polishing cloth. To remove residual polishing material, electrode was rinsed with methanol followed by deionised water and sonicated for 2 min. First, different concentrations of Bi_2O_3 and MWCNTs were prepared in N,N-dimethylformamide (DMF) under ultrasonication for 30 min at room temperature. Then MWCNTs, 1 mg mL^{-1} and Bi_2O_3, 2 mg mL^{-1} were selected as optimum based on the current response of cilostazol at fixed concentration. On the basis of higher current response mixture of Bi_2O_3 and MWCNTs were prepared in the ratio of 2:1 by same procedure. The modified electrodes, Bi_2O_3/GCE, MWCNTs/GCE, and Bi_2O_3–MWCNTs/GCE were prepared by drop coating of 10 μL of respective suspension at the GCE surface using a micropipette and left for drying at room temperature. After electrochemical measurement film was removed mechanically from the surface of the GCE.

3 Results and discussion

3.1 Surface characterization of Bi_2O_3/GCE, MWCNTs/GCE, and Bi_2O_3–MWCNTs/GCE

The surface morphology of the Bi_2O_3/GCE, MWCNTs/GCE, and Bi_2O_3–MWCNTs/GCE were characterized through SEM by mechanical attached and evaporated technique on a glassy carbon electrode using Philips SCI quanta 400 instrument. Scanning electron micrograph is shown in Fig. 1. It can be seen that the Bi_2O_3 were seen in the spherical form (Fig. 1a), MWCNTs were seen in tubes form (Fig. 1b), which are twisted together and Bi_2O_3–MWCNTs were seen as twisted form of both spherical and tubes (Fig. 1c).

3.2 Voltammetric behavior of Bi_2O_3/GCE, MWCNTs/GCE, Bi_2O_3–MWCNT/GCE and comparison with bare GCE

3.2.1 Cyclic voltammetry

Cyclic voltammetry is one of the widely used techniques providing the considerable information about the reversibility of the redox reaction. To accomplish this purpose, the electrochemical response of a solution of cilostazol (10 μg mL^{-1}) was examined in the potential range 0.2–1.6 V (vs. Ag/AgCl) by initiating the sweep in positive and negative direction. A well-defined oxidation peak is observed when the sweep was initiated in the positive direction and no other peak noticed in the voltammogram. Cilostazol showed a single well-defined irreversible anodic peak at both GCE and modified electrodes. The cyclic voltammograms of cilostazol showed 1.4 times enhancement in the oxidation peak current at Bi_2O_3/GCE, 2.0 times

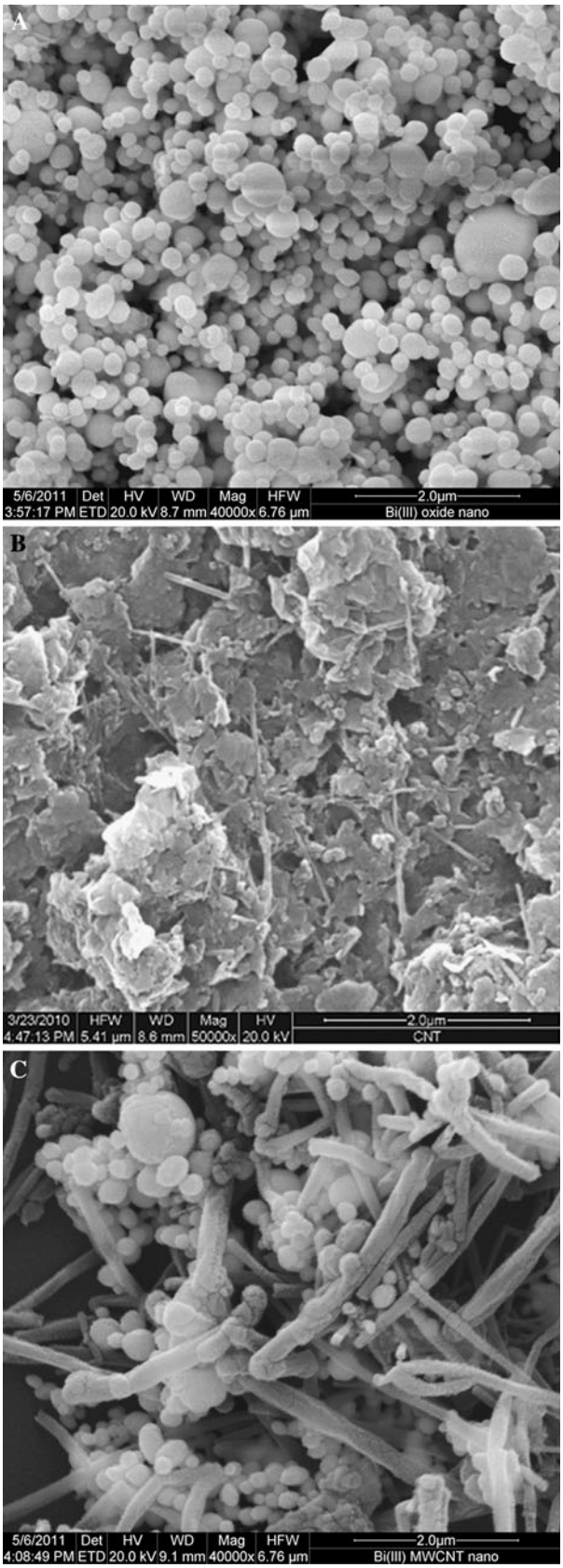

Fig. 1 Scanning electron microscopy of Bi_2O_3 (**a**) MWCNTs (**b**), and mixture of Bi_2O_3–MWCNTs (**c**)

enhancement at MWCNTs/GCE, and 3.3 times enhancement at Bi_2O_3–MWCNTs/GCE as compared to a bare GCE, Fig. 2 (curve c–e and b respectively).

Figure 2 showed that the peak potential obtained at the Bi_2O_3/GCE, MWCNTs/GCE, and Bi_2O_3–MWCNTs/GCE was shifted left hand side with potential, 20, 40, and 42 mV, respectively, as compared with the bare GCE. These results indicated that the electrochemical oxidation of cilostazol are probably the same, i.e. at the modified GCE and at the bare GCE, and the electron transfer kinetics was slightly higher in the case of modified electrode, therefore somewhat improving the sensitivity for voltammetric measurement.

3.2.2 *Square-wave voltammetry*

Square-wave voltammograms were recorded for cilostazol (10 μg mL^{-1}) in the potential range 0.2–1.6 V (vs. Ag/AgCl). Cilostazol showed a single well-defined anodic peak at both GCE and modified electrodes. The square-wave voltammograms showed 1.3 times enhancement at Bi_2O_3/GCE, 2.4 times enhancement at MWCNT/GCE and 4.9 times enhancement at Bi_2O_3–MWCNTs/GCE as compared to a bare GCE, Fig. 3 (curve b–d and a respectively).

Figure 3 showed that the peak potential obtained at the Bi_2O_3/GCE, MWCNTs/GCE, and Bi_2O_3–MWCNTs/GCE was also shifted left hand side with potential, 30, 90, and 78 mV, respectively, as compared with the bare GCE. Thus, the increase in peak current response along with the lowering of peak potential is a clear evidence of higher sensitivity of the to Bi_2O_3–MWCNT/GCE sensor, that is why it is used for quantitative measurements.

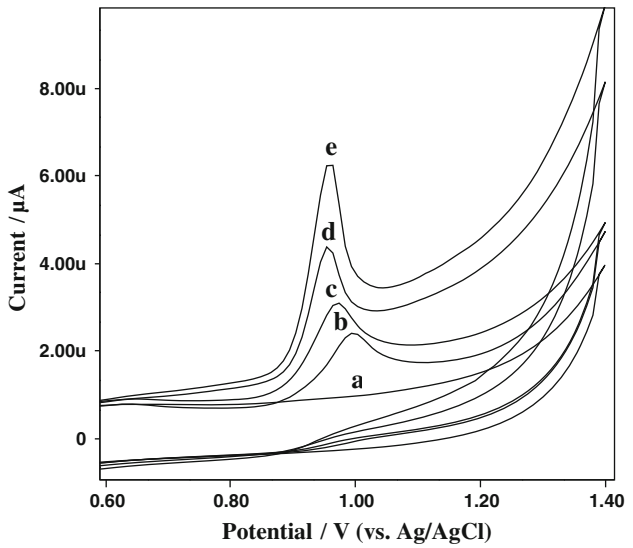

Fig. 2 Cyclic voltammograms of cilostazol (10 μg mL^{-1}) at Bi_2O_3–MWCNTs/GCE (curve *e*), MWCNTs/GCE (curve *d*), Bi_2O_3/GCE (curve *c*), bare GCE (curve *b*), and blank (curve *a*)

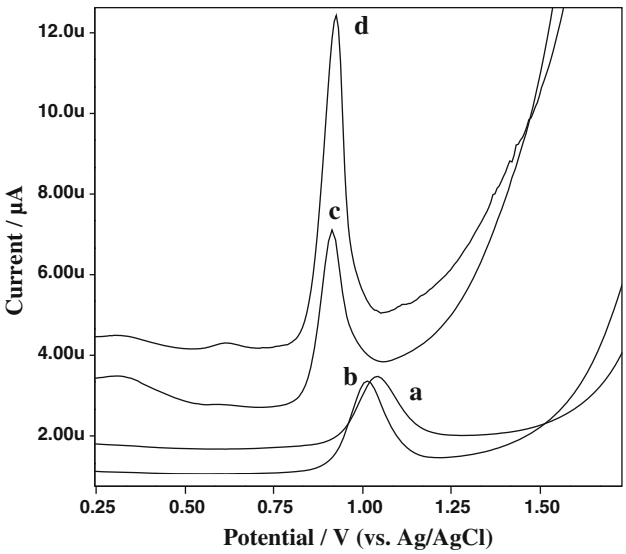

Fig. 3 Square-wave voltammograms of cilostazol (10 μg mL^{-1}) at Bi_2O_3–MWCNTs/GCE (curve *d*), MWCNTs/GCE (curve *c*), Bi_2O_3/GCE (curve *b*), and bare GCE (curve *a*)

3.3 Effect of supporting electrolyte and pH

The characteristics of voltammogram were dependent on various electrolytes and pH of the medium. Various supporting electrolytes such as KCl, phosphate buffer, acetate buffer, borate buffer, and BR buffer were examined. Cilostazol gave well-defined oxidation peaks in BR buffered solution. In order to achieve optimum pH value for the anodic oxidation of cilostazol on the surface of modified electrode, the electrochemical behavior was investigated in pH range 2.5–12.0 at constant concentration. Optimum peak current was achieved at pH 2.5, with the rise in pH the peak current decreases due to pH dependence of half wave potential which indicates the involvement of protons in the electrode process and finally dislocated as we moved toward more alkaline pH due to lower number of available protons. With the rise in pH peak potential was also shifted toward negative side. The linear dependence of peak potential on pH can be expressed by the following relation:

$$E_P/\text{mV (vs. Ag/AgCl)} = 1.094 - 0.350\ \text{pH} \quad (1)$$

3.4 Effect of scan rate

The effects of varying scan rates (v) on the peak current (i_p/μA) of cilostazol in BR buffer solution (pH 2.5) were studied over 25–250 mV s^{-1}. As the scan rate were increases from 25 to 250 mV s^{-1} at a fixed concentration of cilostazol, the peak potential shifted toward right hand side accompanying the increase in current values, Fig. 4 (a, curves b–k), thus confirming the irreversible nature of the oxidation process of cilostazol. The plot of i_p vs. $v^{1/2}$ (Fig. 4b) indicated that the reaction occurring at the surface

of modified electrode is governed by the diffusion process [51, 52]. The dependence of peak current on scan rate can be expressed by following equation:

$$i_p/\mu A = 0.2355\,(v^{1/2}, \text{mV s}^{-1}) + 0.4068;\ r^2 = 0.9839 \quad (2)$$

3.5 Effect of cilostazol concentrations and detection limit

The Bi_2O_3–MWCNTs/GCE was introduced for the determination of cilostazol through square-wave voltammetric technique. Square-wave voltammograms obtained at the modified electrode showed that, peak current increased linearly with increasing concentration. The linear increase in the peak currents are undoubtedly attributed to the unique characteristics of Bi_2O_3 and MWCNTs nanoparticles. Since the modified electrode greatly improved the sensitivity for the determination of cilostazol, it signifies that Bi_2O_3–MWCNTs/GCE exhibits electrocatalytic activity for the oxidation of cilostazol. Using the optimum conditions described above, linear calibration curve is obtained for cilostazol over the concentration range 0.8–13 μg mL^{-1} (Fig. 5) and may be expressed by the equation:

$$i_p/\mu A = 0.5566\,(\mu g\ mL^{-1}) + 1.3763;\ r^2 = 0.9921 \quad (3)$$

The limit of detection (LOD) estimated as 3 s m^{-1} and limit of quantitation (LOQ) estimated as 10 s m^{-1} was 0.76 and 2.31 μg mL^{-1}, respectively. The analytical characteristics for standard linearity and related validation parameters are also calculated and summarised in Table 1.

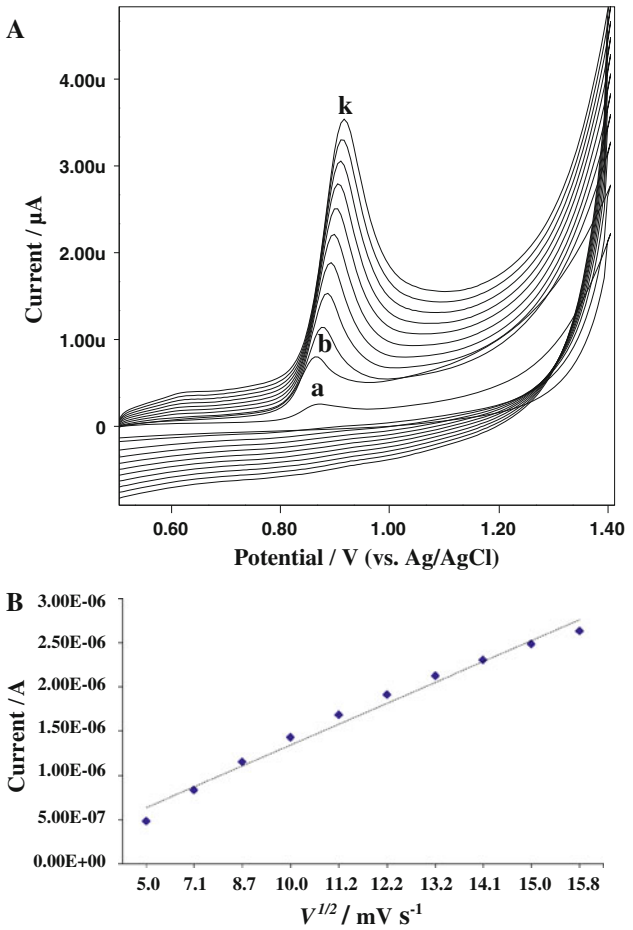

Fig. 4 Cyclic voltammograms of cilostazol (10 μg mL^{-1}) at sweep rates 25–250 mV s^{-1} (**a**, curves *b–k*) and blank solution (**a**, curve *a*) and plot of sweep rate versus current (**b**)

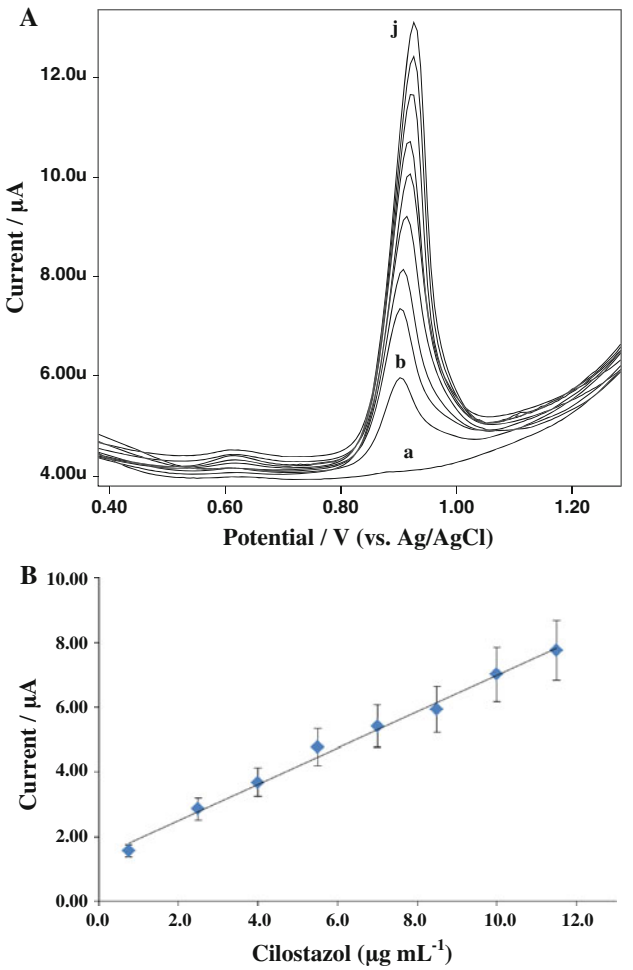

Fig. 5 Square-wave voltammograms of cilostazol at Bi_2O_3–MWCNTs/GCE at concentration levels, 0.8–13 μg mL^{-1} (**a**, curves *b–j*), blank solution (**a**, curve *a*) and plot of concentration versus peak current of cilostazol standard solution (**b**)

Table 1 Square-wave voltammetric method validation parameters for standard linearity

Linearity parameters	Standard	Plasma
Slope	0.5509	0.1448
Standard deviation	0.0159	0.0037
Intercept	1.4309	0.5712
Standard deviation	0.1272	0.0291
Correlation coefficient	0.9942	0.9974
Standard error of estimation	0.1869	0.0378
Sum of squares of regression	41.9049	2.2175
Sum of squares of residuals	0.2444	0.0057
Limit of detection (μg mL^{-1})	0.76	0.66
Limit of quantification (μg mL^{-1})	2.31	2.01

3.6 Analytical application of Bi_2O_3–MWCNTs/GCE

3.6.1 Determination in pharmaceutical formulation

The reliability of the Bi_2O_3–MWCNTs/GCE was examined by applying square-wave voltammetric method for the determination of cilostazol drug in the real samples (commercial dosage form, Tablet *Pletoz*®)). For this ten tablets of cilostazol (*Pletoz*® 50 mg/Tab) were crushed to fine powder and all contents were mixed properly. For preparation of a test stock solution (1 mg mL^{-1}) sufficient amount of the crushed tablets equivalent to 25 mg of cilostazol was taken into 25-mL volumetric flask and volume was made up to mark with acetonitrile. Solution was sonicated for 5 min to dissolve all contents of tablets properly and centrifuged at 3,200 rpm for 5 min. After that, clear supernatant liquid of test solution was withdrawn and diluted with same solvent to achieve concentration fall in the range of calibration curve. The square-wave voltammograms were then recorded under identical conditions which were used during plotting the calibration curve. The mean results were found very closer to the nominal value. The results indicated that proposed electrode was successfully applied for quantification of cilostazol in pharmaceutical formulation (Table 2).

3.6.2 Determination in spiked human plasma

The proposed method was successfully applied for the determination of cilostazol in spiked human plasma samples. Acetonitrile was used as a protein-precipitating agent for extraction of cilostazol from spiked plasma samples. The analyses were carried out without the necessity for the sample pre-treatment or time consuming extraction purification steps, other than single step protein precipitation followed by centrifugation. The voltammograms were recorded under identical condition described in Sect. 2.3

Table 2 Determination of cilostazol in tablets (*Pletoz*®) by the proposed voltammetric methods

Amount added (μg)	Amount found[a] (μg)	Accuracy (%)	CV (%)	Error (%)
3.0	2.98	99.33	1.98	−0.67
7.0	6.97	99.57	0.92	−0.43
10.0	9.99	99.90	1.04	−0.10

[a] Amount found represents average of six observations ($n = 6$)

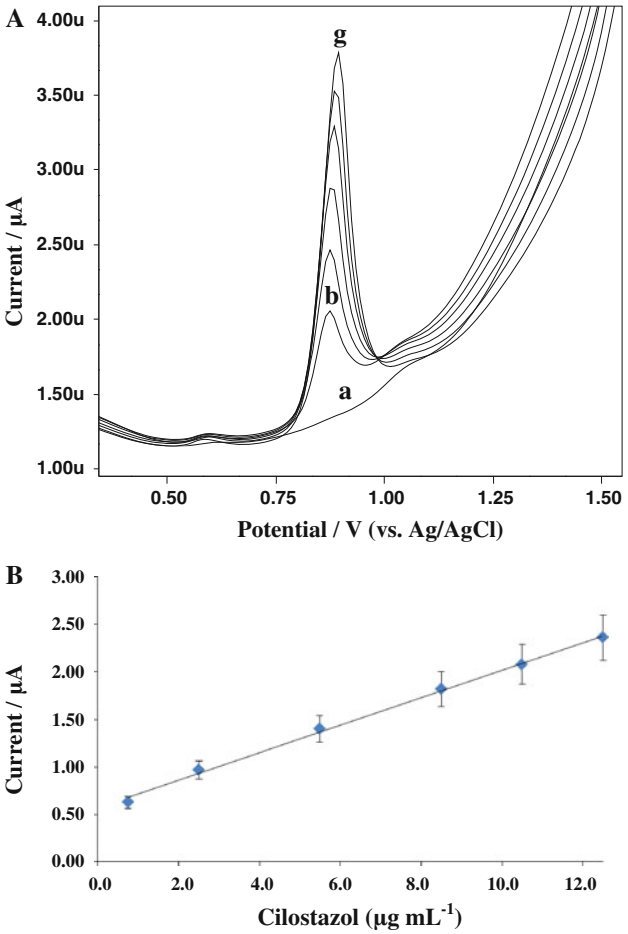

Fig. 6 Square-wave voltammograms of cilostazol extracted from plasma at Bi_2O_3–MWCNTs/GCE at concentration levels, 0.8–12.5 μg mL^{-1} (**a**, curves *b*–*g*), blank solution (**a**, curve *a*) and plot of concentration versus peak current of cilostazol extracted from plasma (**b**)

using Bi_2O_3–MWCNTs/GCE. An excellent calibration curve was obtained over a wide concentration range 0.8–12.5 μg mL^{-1} (six concentration levels) with good correlation coefficient (r^2) of 0.9974. The calibration plot resulted in a straight line expressed by the equation:

$$i_p/\mu A = 0.1448\left(\mu g\ mL^{-1}\right) + 0.5712 \quad (4)$$

Representative voltammograms with different concentrations of cilostazol extracted from human plasma

Table 3 Determination of cilostazol extracted from human plasma using protein precipitation techniques

Amount added (μg)	Amount extracted[a] (μg)	Accuracy (%)	CV (%)	Error (%)
3.0	2.96	98.67	1.22	−1.33
7.0	6.94	99.14	1.48	−0.86
10.0	9.94	99.40	1.13	−0.60

[a] Amount extracted represents average of six observations ($n = 6$)

samples are shown in Fig. 6a and its calibration curve shown in Fig. 6b. No interfering peaks were observed at the potential of analyte Fig. 6a, curve a indicated the specific nature of the electrode. Various statistical parameters for linear regression equation were also calculated and reported in Table 1. Limit of detection 0.66 μg mL^{-1} and limit of quantification 2.01 μg mL^{-1} were achieved by means of square-wave voltammetric methods, which proved the sensitivity of the method. The amount of cilostazol extracted from human plasma using protein precipitation techniques are summarized in Table 3. The results indicated good accuracy and precision of the proposed method.

4 Conclusion

The Bi_2O_3/GCE, MWCNTs/GCE, and Bi_2O_3–MWCNTs/GCE revealed an electroanalytical performance for the oxidation of cilostazol which was compared favorably with that of the bare GCE. The square-wave and cyclic voltammogram of cilostazol at Bi_2O_3–MWCNTs/GCE showed 4.9 and 3.3 times enhancement in peak currents, respectively, as compared to bare GCE. The main advantage of the Bi_2O_3–MWCNTs/GCE is its favourable surface stability which provides great possibilities for successive voltammetric measurements, whereas in the case of bare GCE needs a tedious polishing of the electrode surface after each measurement. The Bi_2O_3–MWCNTs/GCE seems to be readily applicable for redox measurements. However, apart from the improvement in the sensitivity, its non toxic character, high electrical conductivity, chemical stability, and mechanical strength proved suitable electrochemical sensor for its application in voltammetric measurement.

Acknowledgments The authors are thankful to Cadila Pharmaceuticals Ltd. (India), for providing the standard of cilostazol.

References

1. Durst RA, Baumner AJ, Murray RW, Buck RP, Andrienx CP (1997) Pure Appl Chem 69:1317
2. Radhi MM, Tan WT, Zaki M, Rahman A, Kassim AB (2010) Am J Appl Sci 7:395
3. Nigovic B, Simunic B, Hocevar S (2009) Electrochim Acta 54:5678
4. Zidan M, Tan WT, Zainal Z, Abdullah AH, Goh JK (2010) Int J Electrochem Sci 5:501
5. Wang J (2005) Electroanalysis 17:1341
6. Li L, Yan B (2009) J Alloys Compd 476:624
7. Gujar TP, Shinde VR, Lokhande CD, Mane RS, Han SH (2006) Appl Surf Sci 250:161
8. Economou A (2005) Trends Anal Chem 24:334
9. Kokkinos C, Economou A (2008) Curr Anal Chem 4:183
10. Zidan M, Tan TW, Abdullah AH, Zainal Z, Kheng GJ (2011) Int J Electrochem Sci 6:279
11. Kokkinos C, Economou A, Raptis I, Speliotis T (2011) Electrochem Commun 13:391
12. Wang J, Lu J, Hocevar SB, Ogorevc B (2001) Electroanalysis 13:13
13. Wang J, Lu J, Kirgoz UA, Hocevar SB, Ogorevc B (2001) Anal Chim Acta 434:29
14. Hocevar SB, Wang J, Deo RP, Ogorevc B (2002) Electroanalysis 14:112
15. Vytras K, Svancara I, Metelka R (2002) Electroanalysis 14:1359
16. Krolicka A, Bobrowski A, Kalcher K, Mocak J, Svancara I, Vytras K (2003) Electroanalysis 15:1859
17. Krolicka A, Bobrowski A (2004) Electrochem Commun 6:99
18. Bobrowski A, Novak K, Zarebski J (2005) Anal Bioanal Chem 382:1691
19. Kefala G, Economou A, Voulgaropoulos A (2004) Analyst 129:1082
20. Chatzitheodorou E, Economou A, Voulgaropoulos A (2004) Electroanalysis 16:1745
21. Kruusma J, Banks CE, Compton RG (2004) Anal Bioanal Chem 379:700
22. Maghasi AT, Halsall HB, Heineman WR, Rilo HLR (2004) Anal Biochem 326:183
23. Legeai S, Soropogui K, Cretinon M, Vittori O, Oliveira AHD, Barbier F, Grenier-Loustalot MF (2005) Anal Bioanal Chem 383:839
24. Duwensee H, Adamovski M, Flechsig G (2007) Int J Electrochem Sci 2:498
25. Sattayasamitsathit S, Thavarungkul P, Kanatharana P (2007) Electroanalysis 19:502
26. Ganchimeg P, Tee TW, Yusof NA, Kheng GJ (2011) J Appl Sci 11:848
27. Ganchimeg P, Tee TW, Yusof NA, Kheng GJ (2011) Int J Electrochem Sci 6:520
28. Ribeiro WF, Selva TMG, Lopes IC, Coelho ECS, Lemos SG, Caxico de Abreu F, Bernardo do Nascimento V, Ugulino de Araujo MC (2011) Anal Methods 3:1202
29. Carvalho RC, Gouveia-Caridade C, Brett CM (2010) Anal Bioanal Chem 398:1675
30. Iijima S (1991) Nature 354:56
31. Roche S (2000) Annales de Chimie Science des Materiaux 25:529
32. Rahman MM, Jeon IC (2007) J Braz Chem Soc 18:1150
33. Nguyen CV, Chao KJ, Stevens RMD (2001) Nanotechnology 12:363
34. Li H, Cone J, Fong M, Kambayashi J, Yoshitake M, Liu Y (2005) Cardiovasc Drugs Ther 19:41
35. Tsuchikane E, Katoh O, Sumitsuji S, Fukuhara A, Funamoto M, Otsuji S, Tateyama H, Awata N, Kobayashi T (1998) J Am Heart 135:495
36. Shinoda-Tagawa T, Yamasaki Y, Yoshida Y, Kajimoto Y, Tsujino T, Hakui N, Matsumoto M, Hori M (2002) Diabetologia 45:188

37. Elam MB, Heckman J, Crouse JR, Hunninghake DB, Herd JA, Davidson M, Gordon IL, Bortey EB, Forbes WP, Ame J (1998) Heart 18:1942
38. Doo H, Cho HY, Lee YB (2010) Br J Clin Pharmacol 69:27
39. Choi JM, Shin HK, Kim KY, Lee JH, Hong KW (2002) J Pharmacol Exp Ther 300:787
40. Nirogi RVS, Kandikere VN, Shukla M, Mudigonda K, Shrivasthava W, Datla PV, Yerramilli A (2006) Anal Bioanal Chem 384:780
41. Jadhav AS, Pathare DB, Shingare MS (2007) Drug Dev Ind Pharm 33:173
42. Tata Prasad NV, Chau-Hwei JF, Bramer SL (2001) J Pharm Biomed Anal 24:381
43. Tata Prasad NV, Chau-Hwei JF, Browder NJ, Chow PC, Bramer SL (1998) J Pharm Biomed Anal 18:441
44. Jain R, Yadav RK, Dwivedi A (2010) Colloids Surf A 359:25
45. Jain R, Gupta VK, Jadon N, Radhapyari K (2010) Anal Biochem 407:79
46. Jain R, Gupta VK, Jadon N, Radhapyari K (2010) J Electroanal Chem 648:20
47. Jain R, Yadav RK (2011) Drug Test Anal 3:171
48. Jain R, Rather JA (2011) Colloids Surf B 83:340
49. Jain R, Rather JA (2011) Colloids Surf A 378:27
50. Jain R, Rather JA, Dwivedi A, Vikas (2010) Electroanalysis 22:2600
51. Wopschall RH, Shain I (1967) Anal Chem 39:1527
52. Quente F, Elleouet C (2001) Electroanalysis 13:1030